Research paper

Measurement and modelling of the temperature distribution caused by the heat of cement hydration

Andrzej Helowicz[1]

Abstract: This paper describes the author's method for the direct and continuous measurement of the temperature distribution during the initial period of hardening concrete, together with the results of tests obtained with its use. The first successful test using this method was conducted by the author in May 2001 [7]. In the following years, the author successfully used this method in the study of other structural elements [8] and [9]. He independently developed and made the necessary elements to measure the temperature in hardening concrete. The tested element is a reinforced concrete column with a diameter of 2.0 m and a height of 8.0 m, which is an intermediate support for the flyover under construction along the Wrocław city ring road. The structure consists of two independent continuous 15-span structures made of pre-stressed concrete (Fig. 1). The article additionally presents numerical model of the previously tested reinforced concrete pillar and the calculation results obtained. The numerical calculations were carried out using the Abaqus FEA software [1]. In conclusions, the author summarises the important elements of the on-site test and makes recommendations for further use of this method to predict the temperature distribution in other elements of the structure, provided that they are made of exactly the same concrete mixture.

Keywords: mass concrete, cement, measurement and modelling, heat generated by cement hydration

[1]PhD., Eng., Wrocław University of Science and Technology, Faculty of Civil Engineering, Na Grobli 15, 50-421 Wrocław, Poland, e-mail: andrzej.helowicz@pwr.edu.pl, ORCID: 0000-0001-9527-1281

1. Introduction

The paper describes the author's method for the direct and continuous measurement of the temperature distribution during the initial period of hardening concrete, together with the results of tests obtained with its use. The first successful test using this method was conducted by the author in May 2001 [7]. In the following years, the author successfully used this method in the study of other structural elements [8]. He independently developed and made the necessary elements to measure the temperature in hardening concrete. He carried out multiple tests on a real element of the bridge structure. Furthermore, in the Abaqus FEA software [1] a numerical model of the reinforced concrete column was built, taking into account thermal processes such as conduction and convection. In the numerical model, the influence of thermal radiation was omitted due to the small influence of radiation on the distribution of temperature fields in the tested element.

The numerical model uses the kinetics of heat hydration release as a function of time for the WARTA cement used to make the real column and the air temperature measured during the on-site tests conducted on this column. Laboratory test of the total amount of heat hydration generated in 1 g of cement was obtained from the WARTA cement plant [19]. The tested element is a reinforced concrete column with a diameter of 2.0 m and a height of 8.0 m, which is an intermediate support for the flyover under construction along the Wrocław city ring road. The flyover deck cross-section is presented in Fig. 1.
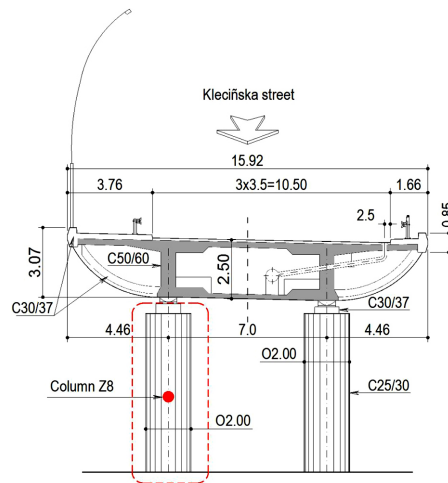

Fig. 1. The flyover deck cross-section through the western line with tested column

The flyover consists of two independent continuous 15-span structures made of pre-stressed concrete. The results obtained during the test and from the numerical calculations are summarised in figures and in a table. In conclusions, the author summarises the important elements of the on-site test and makes recommendations for further use of this method to predict the temperature distribution in other elements of the structure, provided that they are made of exactly the same concrete mixture.

2. Research conducted and results

It is important to clarify that the exothermic chemical reaction between cement and water generates the heat of hydration in the hardening concrete. Due to the heat exchange between the hardening concrete and the external environment, time-varying non-uniform temperature fields are generated. As a consequence of the non-uniform temperature distribution, the concrete element deforms, resulting in self-balancing thermal stresses, for example: a free concrete block. Tensile stress appears in the outer layer of the element and compressive stress appear on its inner layer. If the tensile strength of the material is exceeded or the material's capacity for further deformation is exceeded, cracks will appear in the outer layer of the element or in the worst case, the cracks may extend through the entire cross-section of the element. This simple example shows one of the many possible mechanisms that can cause concrete elements to crack or break during concrete hardening. For this reason, it is important to properly control this process in order to limit the peak temperature value and the temperature gradient between its outer and inner layers. This problem has been the subject of many works, to mention just a few [2–14, 16, 20]. However, the experimental data collected are not fully sufficient to identify theoretical models of the phenomenon, especially in the case of high-performance concretes. In addition, it is particularly important in the construction of massive concrete elements such as; a reactor block of the nuclear power plant, a hydroelectric dam structure and a bridge support foundation. For this reason, it is important to collect as many tests as possible carried out on real massive concrete elements in order to correctly perform the numerical modelling of this process. For this purpose, a test was developed and performed on a massive real element of the bridge structure. To measure the internal temperature, the UPM 60 measuring device from Hottinger Baldwin Messtechnik was used (Fig. 2), with PT100 temperature sensors (Fig. 3) placed directly in a specially constructed measuring beam.

Fig. 2. The UPM 60 Hottinger Baldwin Messtechnik measuring apparatus

The location of this beam with the temperature sensors in the column tested on-site is shown in Fig. 4.

The beam was made from a mixture of fine sand and WARTA cement, CEM I MSR 42.5 NA [19]. The same cement was also used to make the element tested on site. The form of the measuring beam was a 2.0 m long PVC plastic pipe with a diameter of 50 mm. In order to embed the cement-sand mixture and the temperature sensors in the form, a 20 mm wide
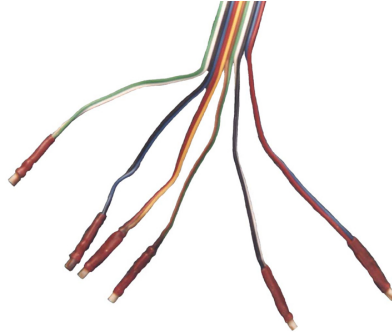
Fig. 3. The PT100 type temperature sensors

Fig. 4. The beam with the PT100 type temperature sensors located inside the column

slot was made along the pipe. The inner surface of the form was coated with a thin layer of silicone spray to avoid its wall sticking to the measuring beam. The beam was reinforced with fiberglass mesh straps. They were placed along the form just before the cement-sand mixture and the temperature sensors were built into it. The fiberglass mesh strips used well protected the measuring beam against damage. To ensure optimal moisture conditions, the measuring beam was covered with a wet cloth for three days. On the fifth day, the form was removed from the measuring beam. The connection of the temperature sensors to the wires was protected with two layers of a heat shrink tube (Fig. 3). Ten PT100 type temperature sensors were placed in the measuring beam. The spacing of these sensors along the length of the beam is shown in Fig. 5.

The checking of the temperature sensors operation was carried out before they were built into the beam and just after the beam was made. The first check consisted of placing all sensors simultaneously in a vessel filled with water and taking a temperature measurement. The measurement read from the UPM 60 measuring apparatus was compared with the reading on the electronic thermometer and with the measurement made with the laboratory mercury thermometer. The temperature difference between the PT100 type temperature sensors and the thermometers did not exceed 1.5°C. Once the form had been removed from the beam, a recheck of the already embedded temperature sensors was carried out. The temperature difference between them did not exceed 1°C. To protect these wires against damage during the
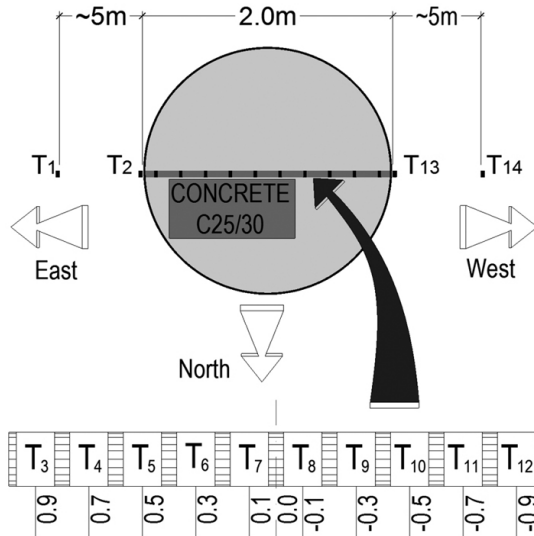
Fig. 5. The position of the beam and the temperature sensors in the column

construction of the column and during the measurements, they were placed in a corrugated plastic tube with a diameter of 20 mm. The measuring beam was placed horizontally halfway up the column and also aligned in an east-west direction (Fig. 5). At time 13:10 the first temperature measurement was made. It was the temperature of the concrete mixture brought to the construction site that covered the measuring beam in the tested column. For safety reasons, the next hardening concrete temperature was taken at 15:09, when the concrete pump left the construction site. It was then possible to connect the UPM 60 measuring apparatus to the power supply cables and the measuring beam. For the first 12 hours, the temperature measurements were taken at intervals of one hour. The subsequent ones took place at intervals of 12 hours. The air temperature measurements T1 and T14 were made with the electronic thermometer, which was previously used to check the operation of the temperature sensors located in the measuring beam. These measurements were carried out in the east-west direction, at which the measuring beam was directed in the tested column. The air temperature measurements were made at a distance of approximately 5 m from the outer surface of the column form and at a height of 2.5 m from the ground surface. The temperature on the outer surface of the form and after its removal on the surface of the columns, at points T2 and T13, were taken using the electronic thermometer at the location of the measuring beam. At each measurement, the temperature of the temperature of the air and the column surface were measured twice. During the tests, on-site the wind speed was not measured. The vertical surface of the column was not subjected to moisture treatment. However, its upper horizontal exposed surface was covered with a layer of geotextile, soaked in water to avoid shrinkage cracking of the concrete. After 72 hours from the end of the concreting, the steel form was removed from the tested column. The form was made of a 5 mm thick steel sheet, which was reinforced with ribs from the same plate, spaced at 0.5 m intervals along the height of the column (Fig. 6).
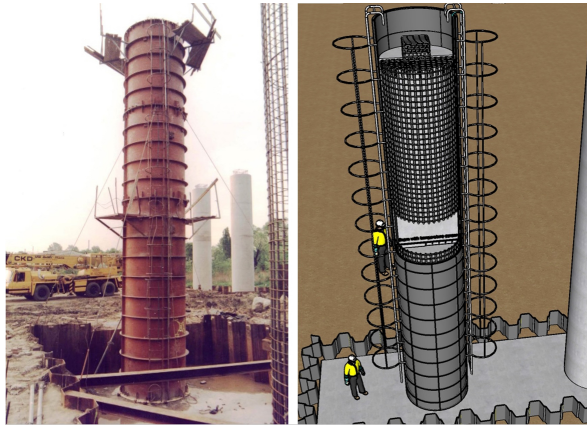
Fig. 6. The column and steel form used to make the column

There was no rain during the testing period. The test was completed 7 days after the first temperature measurement.

3. Description of the numerical model

The numerical model of the column was built in the Abaqus FEA software [1]. Due to the constant cross-section along the column height and the temperature measurements in the middle of its height, a simplified numerical model of the column was built in the two-dimensional Y-Z space (Fig. 7).
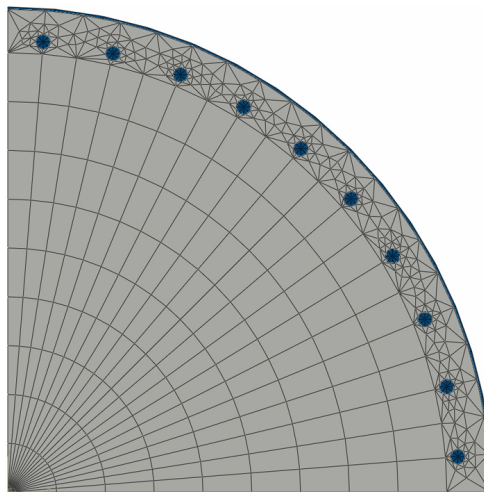

Fig. 7. Numerical model

In addition, the model of the column uses the symmetry of the cross-section with respect to the Y and Z axes. The model consists of three regions. The first region describes a quarter of the concrete column with a diameter of 2 m. The second region is the vertical reinforcement made of bars with a diameter of 32 mm. The third region describes the steel form in the shape of a 5 mm thick plate. The design values of the physical properties for concrete and steel were taken from the European Standard [17] and are presented in Table 1.

Table 1. Material properties used in the numerical model [17]

No.	Material	ρ [kg/m^3]	λ [J/(s·m·K)]	c [J/(kg·K)]
1.	Concrete C25/30	2336	1.7	650
2.	Steel	7800	58	440

ρ – is the mass density, λ – is the coefficient of thermal conductivity, c – is the specific heat capacity

To include the removal of the steel form in the numerical model, the analysis was divided into two steps. In the first step lasting 266400 time increments (74 hours in total), the model consists of three regions; the column, its reinforcement, and the steel form. In the second step lasting 345600 time increments (96 hours in total), the model consists only of the column and its reinforcement. Moreover, in the second step, a model change interaction from the interaction module was introduced in the model in order to deactivate the third region described as the steel form. As a result, the analysis takes into account the removal of the steel form that occurred 74 hours after the start of the on-site testing. Both steps consist of 170 hours spent testing the real structural element. Furthermore, in the first step, between the region of the concrete column and the steel form, a tie constraint type was declared. The tie constraint allows to fuse those two regions. In this constraint, the master surface is the edge of the column region, the secondary surface is the inner edge of the steel form region.

The same type of constraint was applied between the column region and its reinforcement. The model takes into account bidirectional heat transfer in a two-dimensional space, using 4-node linear heat transfer quadrilateral elements type DC2D4 and 3-node linear heat transfer triangle elements type DC2D3 to discretise the regions. For the discretization of the region describing the concrete column, 636 finite elements were used, including 476 triangle elements type DC2D3 and 160 quadrilateral elements type DC2D4. To discretize the region describing the steel bars, eighty triangle finite elements of type DC2D3 were used. Eight triangle elements type DC2D3 per single bar cross-section. Finally, 16 quadrilateral finite elements type DC2D4 were used to discretise the region that describes the steel form. In the heat transfer analysis, the transient heat conduction procedure was used, governed by Fourier's law of heat conduction with a boundary condition defined as surface convection governed by Newton's law of cooling. The tested column was not subjected to strong thermal radiation, so the influence of the thermal radiation was omitted from the analyses. The heat source was the laboratory-measured kinetics of heat of hydration release as a function of time for the WARTA cement CEM I MSR 42.5 NA. This is the same cement that was used to make the column tested on-site (Fig. 8).
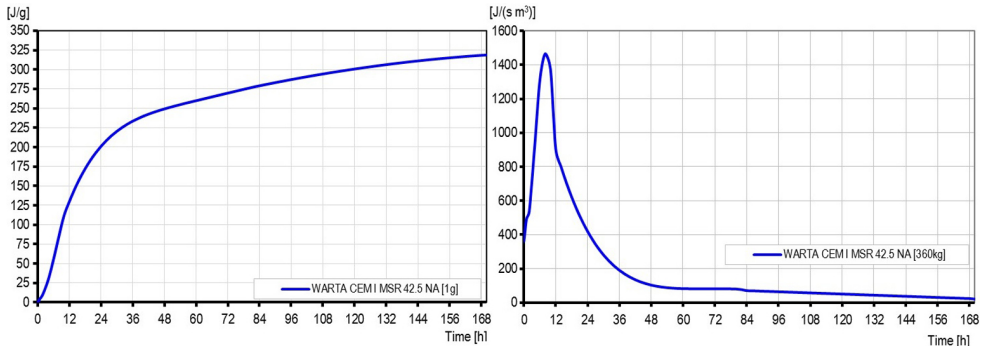
Fig. 8. Kinetics of heat hydration for 360kg of cement as a function of time (170 h)

The hydration heat release as a function of time for the WARTA cement CEM I MSR 42.5 NA was obtained from the WARTA cement plant [19]. The air temperature measured during the on-site tests was input into the numerical model in the convection boundary conditions. The initial measured temperature of the concrete mix, the steel bars and the steel form was defined in the load module as the initial temperature of these regions. The design value of the concrete specific heat in the dry state was changed from 840 to 680 [J/(kg·K)] after preliminary calculations. The design values of the physical properties adopted in the numerical model are given in Table 2. All materials in the analyses were assumed to be isotropic materials. The column tested on-site consists of concrete and in addition a large amount of horizontal circumferential reinforcement made of bars with a diameter of 16 mm. It should be emphasised that the values of the physical properties of steel differ significantly from those of concrete. Therefore, it is difficult to accurately determine the values of the physical properties of a reinforced concrete element in a two-dimensional space. The air temperature was used in the convection boundary conditions. Heat losses were modelled using a constant value of the heat convection coefficient equal to $\alpha = 15$ J/(m^2·s·K).

The composition of the concrete mixture used to make the column is given in Table 2.

Table 2. Concrete mixture

Concrete class C25/30	[kg/m^3]
Cement "WARTA" CEM I MSR 42.5 NA	360
Water (w/c = 0.46)	165.6
Sand 0/2 mm	680.46
Granite grit	1110
Microsilica	14.4

The adopted value of this coefficient corresponds to the wind speed of approximately 2 m/s, acting on the column [11]. Wind speed was not measured during the test and there was also no rain. Both of these factors affect the cooling intensity of the outer surface of

the element and thus increase the undesirable temperature difference between the middle layer and the outer surface of the concrete element. Laboratory-measured the total amount of heat hydration generated in 1 g of WARTA cement, CEM I MSR 42.5 NA is shown in Fig. 8. The right hand side chart shows the kinetics of heat hydration release as a function of time for 360 kg/m^3 of the WARTA cement used in the numerical model. To determine the temperature change in hardening concrete with a time-dependent internal heat source function $Q(t)$, an equation based on Fourier's law of heat conduction was introduced in the Abaqus FEA programme [1], which describes the three-dimensional nonlinear problem of transient heat conduction in an isotropic continuous medium.

This equation takes the form:

$$(3.1) \qquad \frac{\partial T}{\partial t} = \frac{1}{c\rho} \left(\lambda \left(\frac{\partial^2 T}{\partial x^2} + \frac{\partial^2 T}{\partial y^2} + \frac{\partial^2 T}{\partial z^2} \right) + Q \right)$$

in simplified form:

$$(3.2) \qquad \frac{\partial T}{\partial t} = \frac{\left(\lambda \nabla^2 T + Q \right)}{c\rho}$$

where: $T = T(x, y, z)$ – is the medium temperature (the temperature of hardening concrete) [K], t – is the time, [s], λ – is the coefficient of thermal conductivity, depending on the material and temperature [J/(s·m·K)], c – is the specific heat capacity [J/(kg K)], ρ – is the mass density [kg/m^3], $\nabla^2 T$ – is the Laplace operator, $Q(t)$ – is the internal heat source function dependent on time [J/(s·m^3)].

The heat source in this equation is the exothermic chemical reaction of cement and water bonding (Fig. 8). The coefficient of thermal conductivity for materials with a solid specific consistency depends primarily on the temperature. In the case of a liquid concrete mixture composed mainly of loose components such as cement aggregates and water, the values of the physical properties change over time as the concrete hardens [3,10]. Additionally, it is more difficult to accurately determine these parameters for hardening concrete with built-in additional reinforcement. The lack of such data makes it difficult to accurately model the concrete hardening process in the column under study. Therefore, in the numerical model, the initial values of the physical properties of concrete were taken from the European Standard [17]. After the initial calculation of the numerical model, it was necessary to change the specific heat from value 840 to 680 [J/(kg·K)] to match the internal temperatures calculated from the numerical model with those measured in the real column. To describe the heat exchange between the outer surface of the element and the air in the Abaqus FEA software the equation based on Newton's law of cooling was introduced. The column tested on-site was not strongly exposed to solar radiation, and there was no other source of radiation that could significantly affect changes in the temperature fields in the tested column therefore, heat exchange by radiation was omitted in the numerical model. The equation based on Newton's law of cooling takes the form;

$$(3.3) \qquad q_s = \alpha \left(T^s - T_\infty \right)$$

where: q_s – is the heat flux or the rate of heat transfer in or out of the body, [J/(s·m^2)], α – is the convection heat coefficient depending on liquid properties, geometry, wind speed [J/(s·m^2·K)], T^s – is the surface temperature, [K], T_∞ – is the air temperature, [K].

4. The test and calculation results

Figure from 9 to 12 shows the distribution of internal temperatures, measured and computed at the cross-sectional points where the temperature was previously measured during the tests on-site.

In addition, Table 3 lists the main measured temperatures, as well as the time and place of their occurrence.

The research began with measuring the temperature of the concrete mixture delivered to the construction site. Two hours later, after concreting of the column was completed, temperature readings began from temperature sensors placed in the tested column. During on-site tests, the maximum measured internal temperature was 71.9°C. It was measured in the temperature sensor T8 located 10 cm from the centre of the column (Fig. 5). This temperature occurred 31 hours after the start of the test. At the same time, the maximum temperature difference between the temperature sensor T8 and the outer surface of the steel form reached 44.9°C. The largest measured temperature difference between the temperature sensor T8 and the outer
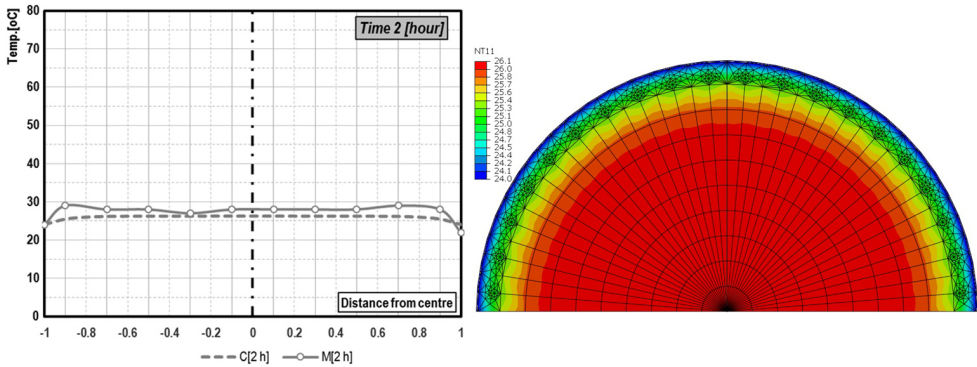

Fig. 9. The temperature distribution across the column after 2 hours of simulation (this is the first reading from the internal temperature sensors)
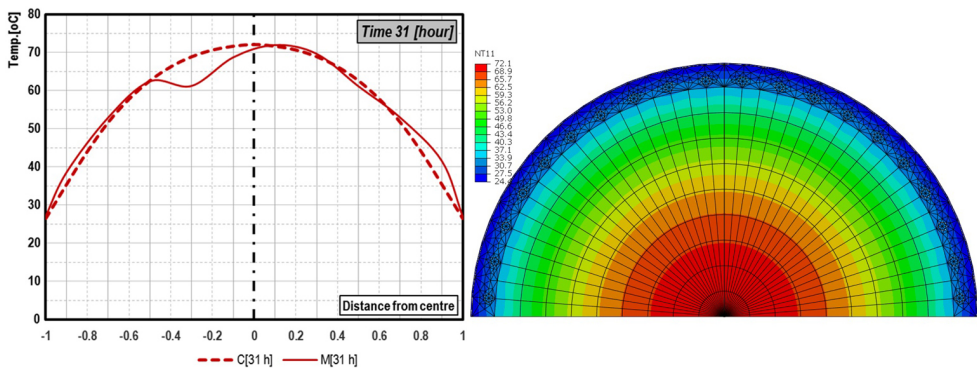

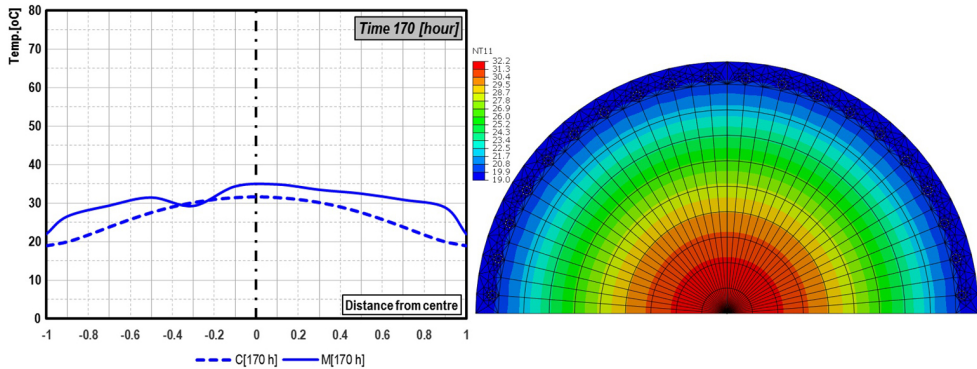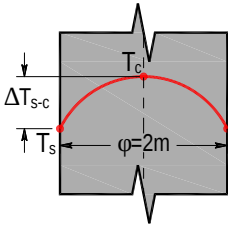Fig. 10. The temperature distribution in the column during the occurrence of the maximum internal temperature

Fig. 11. The temperature distribution across the column at the end of the simulation

Table 3. The main temperatures in the column

Description	Measured temperature & time	Computed temperature & time
Initial temperature of the concrete mix	$T = 24°C$ (0 h)	
Average air temperature	$T_{av.} = 16°C$	
Minimum and maximum air temperature	$T_{min} = 7°C$, $T_{max} = 33°C$	
Maximum temperature in the centre of the column	$T_c = 72°C$ (31 h) $T_c = 35°C$ (170 h)	$T_c = 72°C$ (33 h) $T_c = 32°C$ (170 h)
Maximum temperature difference, between the centre and the surface of the column	$T_{s-c} = 48°C$ (26 h) $T_{s-c} = 13°C$ (170 h)	$T_{s-c} = 49.7°C$ (36 h) $T_{s-c} = 12.7°C$ (170 h)

surface of the steel form was 48°C. This temperature was recorded 26 hours after the start of the tests. The internal temperature gradient increases non-linearly from the centre towards the outer surface of the column. After 170 hours of temperature measurements, the maximum internal temperature measured on the temperature sensor T8 was 34.9°C. At the same time, the measured temperature difference between this sensor and the outer surface of the column was 13°C. During the test, an abnormal temperature measurement was observed on the tem-

perature sensor T6 (Fig. 10 and 12). All temperature measurements from this sensor are clearly lower than the temperature measurement from the twin temperature sensor T9 located symmetrically to the axis of the column. It can be assumed that the T6 temperature sensor was damaged due to high internal stress and temperature in the column. When the influence of the cross-section orientation on the internal temperature values was analysed, lower temperatures were observed in the eastern part than in the western part of the columns. The test shows that
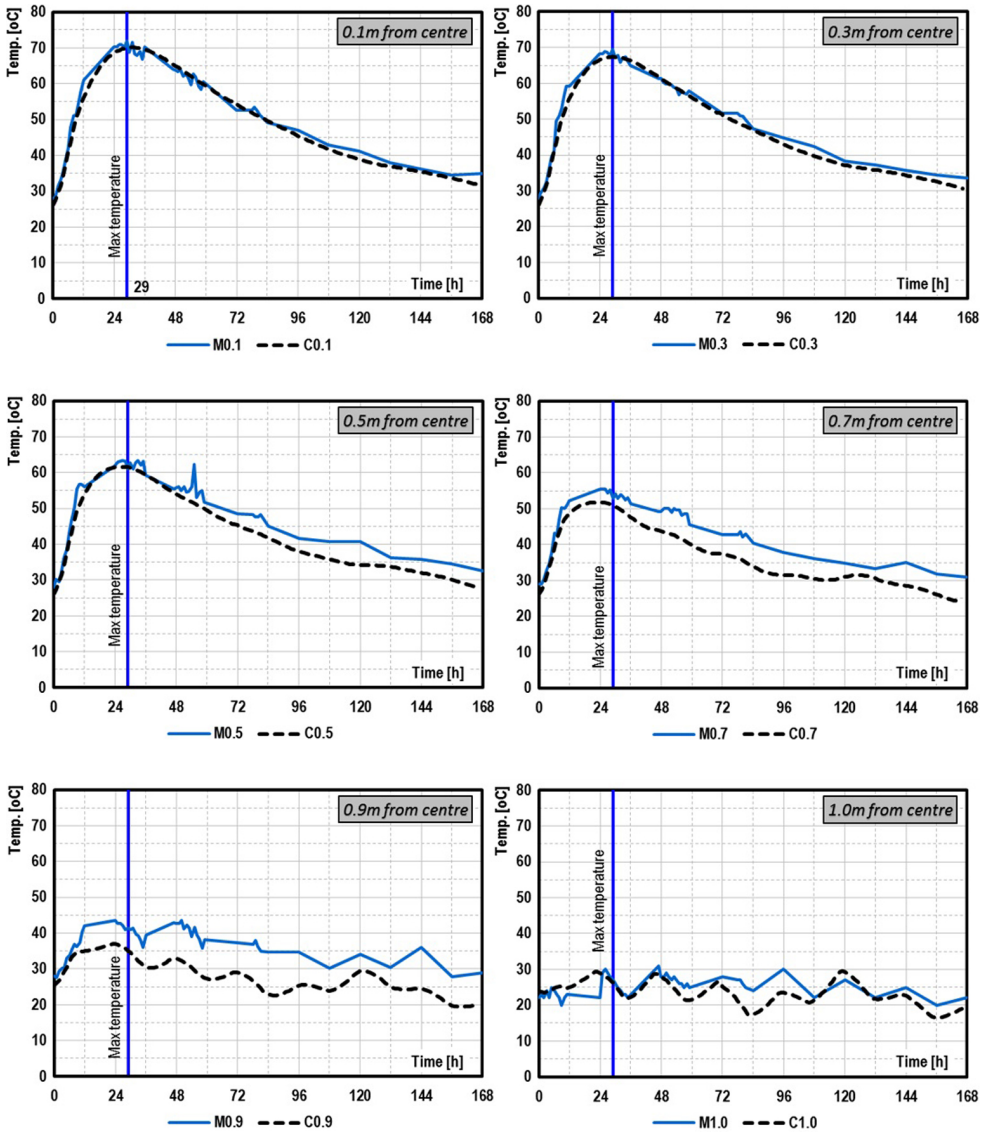

Fig. 12. The temperature values as a function of time

the internal temperature distribution is not symmetric, despite similar air temperatures on both sides of the column. Daily changes in air temperature significantly affect the temperature in the 20 cm thick near-surface layer of the column. The lowest, average and highest measured air temperatures were 7°C, 16°C and 33°C. The time of occurrence of the maximum temperature of the hardening concrete was similar for the measurement and calculation (31 hour & 33 hour). Furthermore, transport of the concrete mixture to the construction site took approximately 30 minutes. The average temperature of the concrete mixture embedded in the column was 24°C. The concreting of the entire column took about 2 hours. The removal of the steel form did not significantly affect the temperature drop on the column surface. This means that the steel form is a very weak insulator and in numerical analysis its influence on the considered processes can be neglected. Table 3 shows a summary of the measured and computed temperatures and their differences with the given time of their occurrence.

When the steel form was removed, no visible damage was observed on the surface of the column.

5. Conclusions

The method proposed by the author for direct and continuous measurement of the temperature distribution made it possible to measure the temperature fields in the massive concrete element during hardening of the concrete. The experimental data bring closer the identification of theoretical models that describe heat transfer during hardening concrete, especially in the case of high-performance concretes. These data, in particular, allowed to determine the maximum internal temperature and temperature difference and the time of their occurrence. Measured large increase in the internal temperature of 48°C in just 26 hours from the start of concrete pouring shows how important the hardening concrete process is for the durability of massive concrete elements. The high temperature gradients recorded during the tests could have caused partial degradation of the young concrete. Small cracks with a width not exceeding the limit value for concrete elements [18] were visible on the surface of the tested column. The tested element did not break. It can only be assumed that the high temperature gradients created during the early maturation period of the young elasto-plastic concrete contributed to the formation of external and internal cracks, which may still have undergone the concrete's self-healing process. The column where the temperature was measured has not cracked or brake to this day. The column is one of the structural elements of the road flyover, which has been in service for many years. The conducted research made the flyover contractor aware of the possible risks associated with high internal temperature gradients during concrete setting in a massive reinforced concrete element that could contribute to damage to the element being made. It can be assumed that a numerical model adjusted in this way can be used to determine the appropriate technology for the construction of other concrete elements, e.g. the remaining columns of the flyover. More research needs to be done on real structural elements to confirm this statement. During the test, wind speed was not measured. Its speed significantly influences the cooling intensity, in particular of the outer layers of the test column. Gauges measuring wind speed should be placed around the tested column to more accurately determine the

effect of wind speed on internal temperatures distribution. The lack of wind speed data is one of the factors responsible for the apparent discrepancies in the temperatures measured and those obtained from the numerical model and the time of their occurrence. In addition, the intensity of the hydration process depends on the specific properties of the binder (clinker mineralogical composition, clinker grinding degree, gypsum content, slag content, pozzolanic additives, additives and admixtures) and temperature. The presented numerical model does not take those factors into account.

During research, frequent temperature measurements are necessary to capture the maximum internal temperature and the temperature difference, as well as when and where they occur. In the case of the tested element, it was impossible to conduct the test remotely due to technological reasons, including the disassembly of the steel form, the waterproofing of the foundation and ongoing construction works in the vicinity of the column. As a consequence, on the first day of the test, it was necessary to be on-site for 18 hours to install the beam with temperature sensors in the column and measure the temperature of the hardening concrete every hour. For the next six days of the test, temperature readings were taken in a twelve-hour cycle. Good access to the construction site made it possible to deliver the measuring apparatus directly to the tested column. The outdoor test required that the measuring apparatus be assembled and disassembled each time. Favourable weather conditions, such as lack of rain and lack of strong wind, facilitated the test, because there was no need to protect the measuring apparatus and electrical cables from adverse weather conditions.

Acknowledgements

References

[1] Abaqus FEA Software, "Abaqus analysis user's manual", Version 2016, Dassault Systemes. [Online]. Available: http://130.149.89.49:2080/v2016/index.html. [Accessed: 01. Aug. 2023].

[2] P.B. Bamforth, *Early-age thermal crack control in concrete*. London, UK: CIRIA, 2007.

[3] A. Długosz, I. Pokorska, R. Jaskulski, et al., "Evolutionary identification method for determining thermophysical parameters of hardening concrete", *Archives of Civil and Mechanical Engineering*, vol. 21, art. no. 35, 2021, doi: 10.1007/s43452-020-00154-7.

[4] K. Flaga, "Wpływ naprężeń własnych na destrukcję naprężeniową i parametry wytrzymałościowe betonu", *Inżynieria i Budownictwo*, no. 6, pp. 315–322, 1995.

[5] K. Flaga, "Wpływ ciepła hydratacji cementu na możliwość zarysowania konstrukcji żelbetowych o rozwiniętym przekroju poprzecznym", *Inżynieria i Budownictwo*, no. 5, pp. 243–245, 1998.

[6] K. Flaga, "Skurcz betonu a trwałość mostów betonowych", *Inżynieria i Budownictwo*, vol. 7-8, 1988.

[7] A. Helowicz, "Rozkład temperatury twardnienia betonu w masywnych elementach obiektu mostowego", *Inżynieria i Budownictwo,* vol. 3-4, pp. 204–207, 2002.

[8] A. Helowicz and J. Biliszczuk, "Pomiar temperatury wiązania betonu B35 w ławie fundamentowej Mostu Milenijnego we Wrocławiu", *Raporty Instytutu Inżynierii Lądowej Politechniki Wrocławskiej, Seria SPR*, vol. 56, 2003.

[9] A. Helowicz, "Analiza pól temperatury wywołanych ciepłem hydratacji w masywach betonowych", PhD thesis, Wrocław University of Technology, 2003.

[10] G. Knor, R. Jaskulski, M.A. Glinicki, et al., "Numerical identification of the thermal properties of early age concrete using inverse heat transfer problem", *Heat and Mass Transfer*, vol. 55, pp. 1215–1227, 2019, doi: 10.1007/s00231-018-2504-2.

[11] W. Kiernożycki, *Betonowe konstrukcje masywne. Teoria wymiarowanie realizacje*. Kraków, Poland: Polski Cement Sp. z o. o., 2003.

[12] W. Kiernożycki, "Niektóre problemy techniczne wykonawstwa betonowych budowli masywnych", *Inżynieria i Budownictwo*, no. 3, 1995.

[13] W. Kiernożycki, J. Ślusarek, and P. Freidenberg, "Temperatury twardnienia betonu wysokowartościowego", *Inżynieria i Budownictwo*, no. 5, 1997.

[14] M. Kucnerowicz-Jakubowska, "Zagadnienia technologii betonu na budowie pochylni Wulkan Nowy Stoczni Szczecińskiej", *Inżynieria i Budownictwo*, no. 5, pp. 278–282, 2001.

[15] A.M. Neville, *Właściwości betonu*. Kraków, Poland: Polski Cement Sp. z o. o., 2000.

[16] L. Ning and L. Guang-Ting, "Time-dependent reliability assessment for mass concrete structures", *Structural Safety*, vol. 21, pp. 23–43, 1999.

[17] ISO 6946 Building components and building elements – Thermal resistance and thermal transmittance – Calculation methods, 2017.

[18] PN-EN 1992-1-1 Projektowanie konstrukcji z betonu. Część 1–1: Reguły ogólne I reguły dla betonów. PKN, 2008.

[19] Warta, cement plant. [Online]. Available: https://www.wartasa.com.pl. [Accessed: 01. Aug. 2023].

[20] P. Witakowski, *Termodynamiczna teoria dojrzewania. Zastosowanie do konstrukcji masywnych z betonu*. Kraków, Poland: Wydawnictwo Uczelniane Politechniki Krakowskiej, 1998.

Pomiar i modelowanie rozkładu temperatury wywołanej ciepłem hydratacji cementu

Słowa kluczowe: beton masywny, cement, pomiar i modelowanie, ciepło hydratacji cementu

Streszczenie:

W artykule opisano autorską metodę bezpośredniego i ciągłego pomiaru rozkładu temperatury w początkowym okresie twardnienia betonu wraz z wynikami badań uzyskanymi przy jej użyciu. Pierwsze udane badanie tą metodą autor przeprowadził w maju 2001 roku. W kolejnych latach autor z powodzeniem stosował tę metodę w badaniach innych elementów konstrukcyjnych. Samodzielnie opracował i wykonał niezbędne elementy do pomiaru temperatury w twardniejącym betonie. Badania przeprowadził na rzeczywistym elemencie konstrukcji mostu. Badanym elementem jest filar żelbetowy o średnicy 2.0 m i wysokości 8.0 m, który stanowi podporę pośrednią budowanej estakady w ciągu obwodnicy Wrocławia. Konstrukcja składa się z dwóch niezależnych ciągłych 15-przęsłowych konstrukcji wykonanych z betonu sprężonego (rysunek 1). W artykule przedstawiono również model numeryczny badanego wcześniej filara żelbetowego i uzyskane wyniki obliczeń. Obliczenia numeryczne wykonano w programie Abaqus. We wnioskach autor podsumowuje istotne elementy badań terenowych i podsumowuje wyniki badań i obliczeń numerycznych oraz podaje zalecenia dalszego wykorzystania tej metody do określenia właściwej technologii wykonania innych elementów betonowych np. pozostałych filarów estakady, pod warunkiem, że są one wykonane z dokładnie tej samej mieszanki betonowej.